Journal of Nuclear Materials 466 (2015) 328–333

Contents lists available at ScienceDirect

Journal of Nuclear Materials

journal homepage: www.elsevier.com/locate/jnucmat

Anti-radiation mechanisms in nanoporous gold studied via molecular dynamics simulations

C.G. Zhang [a], Y.G. Li [a, b], W.H. Zhou [a], L. Hu [a], Z. Zeng [a, b, *]

[a] Key Laboratory for Materials Physics, Institute of Solid State Physics, Chinese Academy of Sciences, Hefei 230031, China
[b] University of Science and Technology of China, Hefei 230026, China

ARTICLE INFO

Article history:
Received 13 March 2015
Received in revised form
26 July 2015
Accepted 2 August 2015
Available online 8 August 2015

Keywords:
Anti-radiation
Molecular dynamics
Nanoporous
Radiation damage

ABSTRACT

The radiation resistance performance of nanoporous (NP) gold is investigated by cascade simulations of a gold nanowire using molecular dynamics. The role of the surface on primary defect production was clarified: the mean size of the vacancy clusters (VCs) near the surface in the nanowire becomes larger compared to that of a single crystal. In the surface region, the reduction of the formation and migration energies of point defects leads to a continuous flux of point defects towards the free surface, which retards the formation and growth of defect clusters, resulting in a good anti-radiation performance. In the cascade region, however, the retained vacancies tend to form larger sessile VCs due to their low migration energies and large attractive forces, resulting in radiation damage. The competition between these two factors determines the anti-radiation behavior of NP gold.

1. Introduction

The irradiation of metals under energetic particles produces a large population of vacancies and self-interstitial atoms (SIAs) [1] that can form clusters, such as dislocation loops [2,3] and voids [4], directly or indirectly. The evolution of these point defects could further lead to amorphization, hardening, or swelling in materials. Therefore, the fusion reactors of the future will require materials that are resistant to extreme radiation conditions without significant changes to their mechanical and thermal properties. Material interfaces can serve as sinks for absorbing and annihilating radiation-induced defects [5–7]. Many experiments have demonstrated that nanostructured materials, such as nanocrystals [8–10], nanolayers [11] and nanoporous (NP) materials [12,13], have superior radiation tolerance compared to their bulk counterparts. Therefore, nanostructured materials are considered to be one of the most promising candidates for the construction materials of nuclear power plants in the future.

NP materials provide a large surface-to-volume ratio due to their three-dimensional open sponge-like structure of interconnected ligaments. Several investigations have focused on the experimental testing [14,15] and computational modeling [16–18] of the mechanical behaviors of NP materials. In general, when materials are subjected to irradiation conditions, a large number of vacancy clusters (VCs) are observed near the surface [19,20] because of the preferential removal of mobile SIAs by free surface. Limited recent studies have been performed on the behavior of NP materials in response to radiation exposure [12,13,21]. With a model and molecular dynamics (MD) simulations, Bringa et al. predicted that the Au NP materials would be resistant to radiation damage over a large dose-rate range [12]. However, these authors only used the diffusivity of point defects to estimate the behavior of defect clusters and did not consider the interactions among the point defects. By using *ex situ* Ne ion irradiation, Fu et al. [21] reported the dose-rate-dependent formation of relatively stable stacking fault tetrahedra (SFT) in nanoporous Au. Sun et al. [13] directly observed the free surface-induced frequent removal of various types of defect clusters, including SFT, individual dislocation loops and dislocation segments in NP Ag subjected to *in situ* Kr ion irradiation. They also indicated that both the global and instantaneous diffusivity of defect clusters in NP Ag are lower compared to those in coarse-grained Ag. Therefore, the behavior of defect clustering is an important factor to understand the enhanced radiation resistance of NP materials. Furthermore, the relation between the numbers of defects generated at the primary damage stage and the distance of the primary knock-on atom (PKA) to the surface is critical to the long-term defect structure evolution.

* Corresponding author. Key Laboratory for Materials Physics, Institute of Solid State Physics, Chinese Academy of Sciences, Hefei 230031, China.
E-mail address: zzeng@theory.issp.ac.cn (Z. Zeng).

http://dx.doi.org/10.1016/j.jnucmat.2015.08.003
0022-3115/

However, to our knowledge, there is no detailed information regarding the distribution of defect clusters in the adjacent region of the surface in NP materials. Therefore, a detailed study is required on the effects of the surface on defect production at the primary damage stage and on the properties of point defects at the long-term evolution stage. In this paper, cascade simulations with energies of 1.0, 1.5 and 2.0 keV are performed at different PKA distances from the surface at 300 K. From the perspective of the thermal behavior of vacancies, the interactions among the vacancies are also analyzed by comparing the energetic parameters and kinetic properties of vacancies between an Au pristine nanowire (NW) and its corresponding cascade NW. Our results indicate that vacancy production is sensitive to the specific distance between the PKA and the surface and exhibits a maximum value versus the distance. The mean size of the interstitial clusters (ICs) becomes smaller; meanwhile, the size of VCs becomes larger. A competition between the two effects of the surface absorption of point defects and vacancies agglomerating in the cascade zone dominates the anti-radiation behavior of NP materials.

2. Methods

2.1. Details of the MD simulations

A single Au NW structure is created to model the influence of radiation damage on Au NP materials. The origin of coordinate is located in the center of the Au NW; the x-axis ⟨100⟩ and y-axis ⟨010⟩ are set along the radial direction, and the z-axis ⟨001⟩ is set along the axial direction; the periodic boundary condition is used along the z-axis. The static relaxed structure of the Au NW with the conjugate gradient method is shown in Fig. 1. The Au embedded atom model (EAM) potential [22] combined with a 'universal' screening function of ZBL [23] at short distances is implemented in the code LAMMPS [24] for our MD simulations. For the EAM potential, the total energy of a system with N atoms is shown as follows:

$$E = \sum_{i}^{N} F(\rho_i) + \frac{1}{2}\sum_{i}^{N}\sum_{j,j\neq i}^{N}\phi(r_{ij}), \tag{1}$$

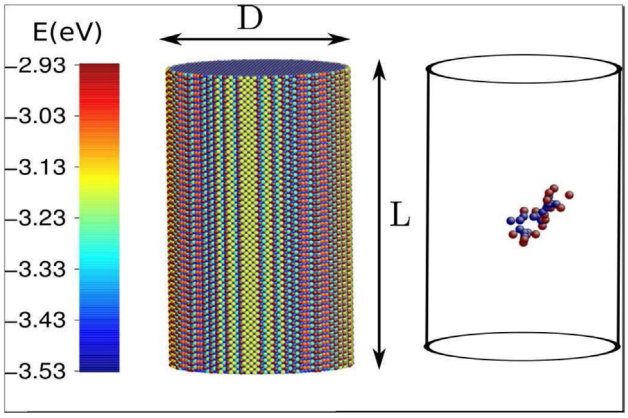

Fig. 1. Visualizations (AtomEye [29]) of the static relaxed Au NW (left) and the configuration of the defects (right) produced by a cascade energy of 2.0 keV after 80 ps of annealing. The diameter (D) and length (L) of the NW are 10.7 nm and 20.4 nm, respectively. In the static relaxed structure, atoms are colored according to their potential energies. In the configuration of the defects, SIAs and vacancies are marked by red and blue colors, respectively. (For interpretation of the references to colour in this figure legend, the reader is referred to the web version of this article.)

where $\phi(r_{ij})$ is the pair-interaction term between atoms i and j separated by the distance r_{ij}, ρ_i is the host electron density at atom i due to the remaining atoms of the system, and $F(\rho_i)$ is the energy to embed atom into the background electron density ρ_i. $\phi(r_{ij})$ can be written as: $e^2/4\pi\varepsilon_0 Z(r_{ij})\cdot Z(r_{ij})/r_{ij}$, where $Z(r_{ij})$ is the effective charge of the pair-interaction term; e and ε_0 are elementary charge and vacuum permittivity, respectively. The effective charge $Z(r_{ij})$ is joined as follows:

$$Z(r_{ij}) = \begin{cases} Z_{ZBL}, & (r_{ij} < r_1) \\ exp\left(b_0 + b_1 r_{ij} + b_2 r_{ij}^2 + b_3 r_{ij}^3\right), & (r_1 \le r_{ij} \le r_2) \\ Z_{EAM-Foiles}, & (r_{ij} > r_2) \end{cases}. \tag{2}$$

When r_1 and r_2 is determined, b_0, b_1, b_2 and b_3 can be determined by controlling $Z(r_{ij})$ and $dZ(r_{ij})/dr_{ij}$ continuous at r_1 and r_2. This combining potential is named as exp-Foiles, whose parameters are shown in Table 1. EAM potentials are widely used for metals because of their accurate description of point defects and surface properties. Another EAM potential developed by Grochola and coworkers [25] is also adopted for comparison. Four different potentials with different joining methods and parameters are applied to compare the results of cascade simulations with energy of 2.0 keV at different PKA distances away from surface of the Au NW. It is found that the tendency of defect production with the PKA distance is nearly the same, so different potentials do not affect the qualitative estimation of the defect production with surface effects. Therefore, the exp-Foiles potential is applied for all calculations in this paper. The MD simulations include two stages. At stage I, the simulation system is relaxed at 300 K with the NVT ensemble (constant number of atoms, volume and temperature) for 10 ps with a time step of 1 fs. At stage II, the NVE ensemble (constant number of atoms, volume and total energy) is applied for 80 ps. At the beginning of this stage, a PKA with a cascade energy of 0.5 keV, 1.0 keV, or 2.0 keV is set at a certain distance from the NW surface. Only the atoms within a shell of approximately 0.4 nm from the outer margin of the NW along the axial direction are under thermostat by applying the velocity rescaling method at 300 K. For all of the MD calculations, the static relaxed Au NW structure is used as an initial configuration and the velocity of the PKA is set along the positive direction of the x-axis. In the following discussion, 'surface' normally refers to the surface region, which is safely defined as 0–0.4 nm from the outer face of the NW according to our defect formation energy analysis. To explore the effects of the initial PKA positions on the defect productions, 11 different PKA distances from the surface are chosen, ranging from 1.27 nm to 9.43 nm, with the same interval of 0.816 nm. To reduce the statistical error, 10 independent cascade simulations are performed at each PKA distance. In addition, for comparison, cascade simulations with energies of up to 30 keV are conducted in a single crystal of Au, and the number of stable defects is obtained, as shown in Fig. A.1. The nudged elastic band method [26] is used to calculate the migration barriers of the point defects for examining the mobility of defects near the surface.

2.2. Defect characteristics

The Wigner–Seitz cells method is used to identify the point defects with reference to the static relaxed Au NW structure. Two

Table 1
The parameters (r_1, r_2, b_0, b_1, b_2, b_3) used for joining ZBL potential and Foiles EAM potential.

$r_1(nm)$	$r_2(nm)$	b_0	b_1	b_2	b_3
0.046716	0.1200	2.8519159	2.8687407	−8.00470296	3.5075770769